

# Histogram Analysis Of Apparent Diffusion Coefficient Maps In Differentiation Of Pediatric Posterior Fossa Tumors

Luis Octavio Tierradentro-Garcia, MD; Jorge Du Ub Kim, MD; Fabrício Guimarães Gonçalves, MD; Alireza Zandifar, MD; Adarsh Ghosh, MD; Dmitry Khrichenko, Savvas Andronikou, MD, PhD; Arastoo Vossough, MD, PhD

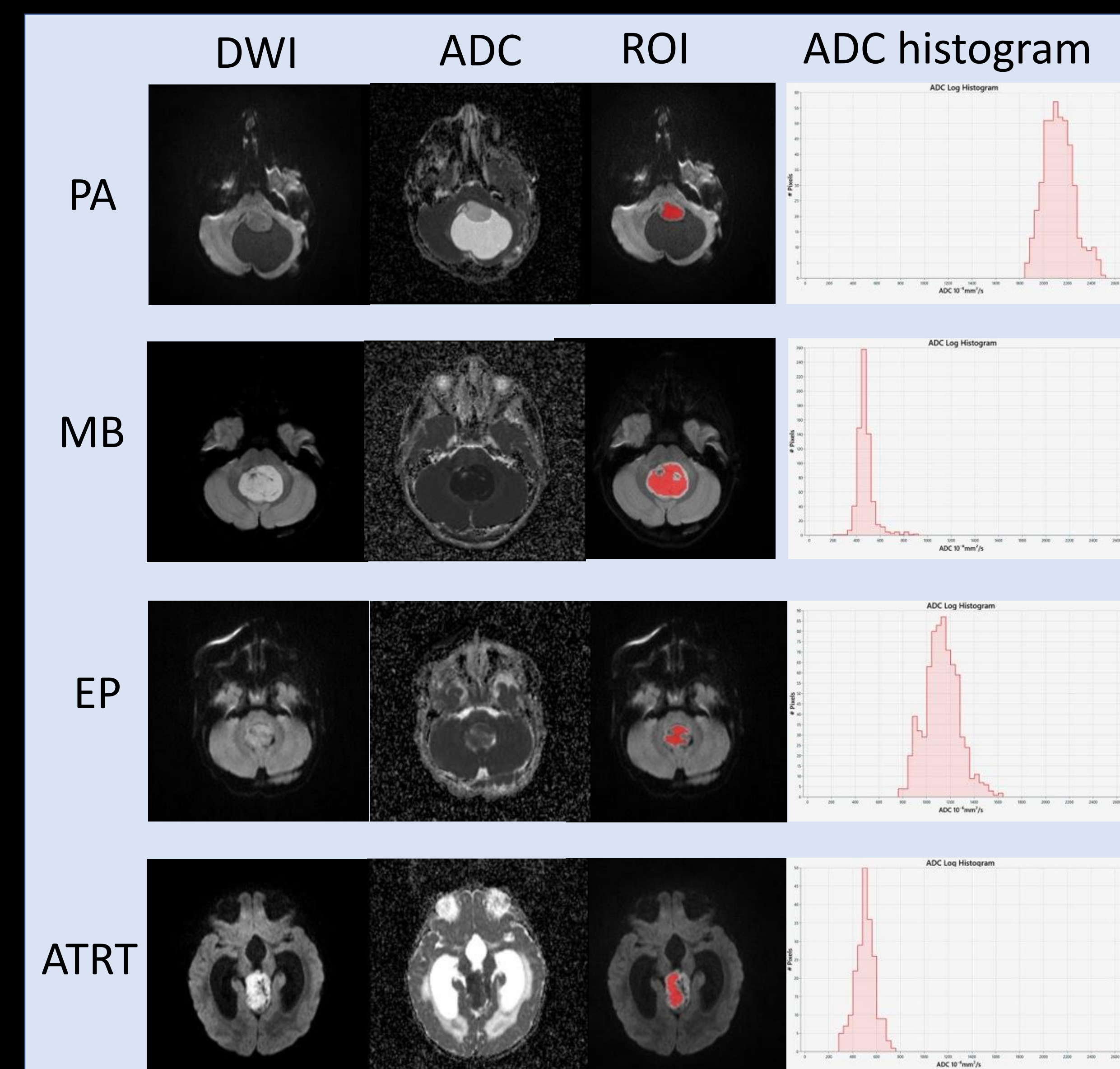
Department of Radiology, Children's Hospital of Philadelphia, Perelman School of Medicine, University of Pennsylvania, Philadelphia, PA, United States of America

## Purpose

This study aimed to evaluate the application of apparent diffusion coefficient (ADC) histogram analysis to differentiate posterior fossa tumors in pediatric patients.

## Methods

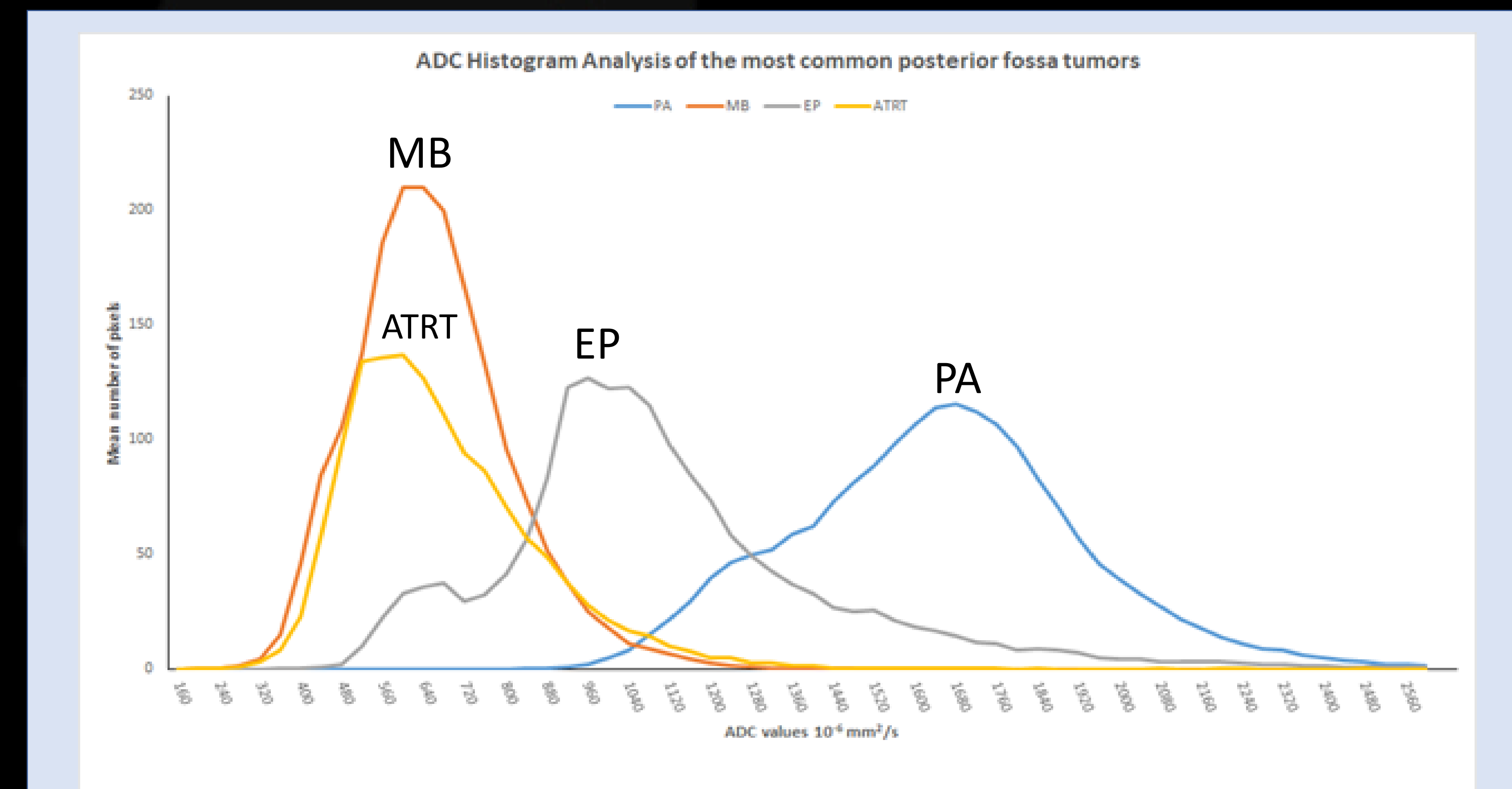
In this retrospective study, we included MRI of 163 pediatric patients with histologically-confirmed posterior fossa tumors, including 75 pilocytic astrocytomas (PA), 59 medulloblastomas (MB), 16 ependymomas (EP) and 13 atypical teratoid rhabdoid tumors (ATRT). DWI sequences were used to manually segment the tumor excluding hemorrhagic, cystic and necrotic elements. Histogram metrics were calculated on a pixel-by-pixel basis. Parametric MRI (pMRI) software was used for segmentation and calculation of the following first-order histogram metrics from ADC maps: entropy, minimum, 10th percentile, 90th percentile, maximum, mean, median, skewness, and kurtosis. Tumor ADC values were normalized to the values of thalamus and cerebellar cortex. The Kruskal Wallis test was used to evaluate the differences in ADC values between the groups. Receiver operating characteristic (ROC) curves were utilized to determine the optimum cutoff values for differentiating the various tumors.



Examples of histograms derived from diffusion weighted imaging and demonstrating regions of interest ROI in children with 4 different tumors: The first row depicts axial brain images of an 11-year-old girl with a diagnosis of posterior fossa pilocytic astrocytoma. The second row shows a 7-year-old boy with classic medulloblastoma. The third row shows a 1-year-old boy with anaplastic ependymoma. The fourth row shows a 1-year-old girl with a diagnosis of atypical teratoid rhabdoid tumor.

## Results

There were significant overall differences in mean, median, 90th percentile, 10th percentile, maximum and minimum ADC values ( $p < 0.001$ ). Post-hoc analysis demonstrated significant pairwise differences of ADC metrics among most tumor types (all  $p < 0.05$  except MB versus ATRT). Normalized ADC data showed similar results to absolute ADC value analysis. For differentiation of EP from MB, mean and median ADC values normalized to thalamus showed an area under the ROC curve (AUC) of 0.985 (95%CI 0.964-1) and 0.982 (95%CI 0.956-1) with a cutoff value of  $>1.067$  for median ADC, demonstrating 93.33% sensitivity and 94.92% specificity. Similarly, mean and median ADC values normalized to the cerebellar cortex demonstrated an AUC of 0.972 (95%CI 0.941-1) and 0.975 (95%CI 0.945-1) with a cutoff value of  $>1.066$  for median ADC, demonstrating 100.00% sensitivity and 88.14% specificity in differentiating EP from MB.



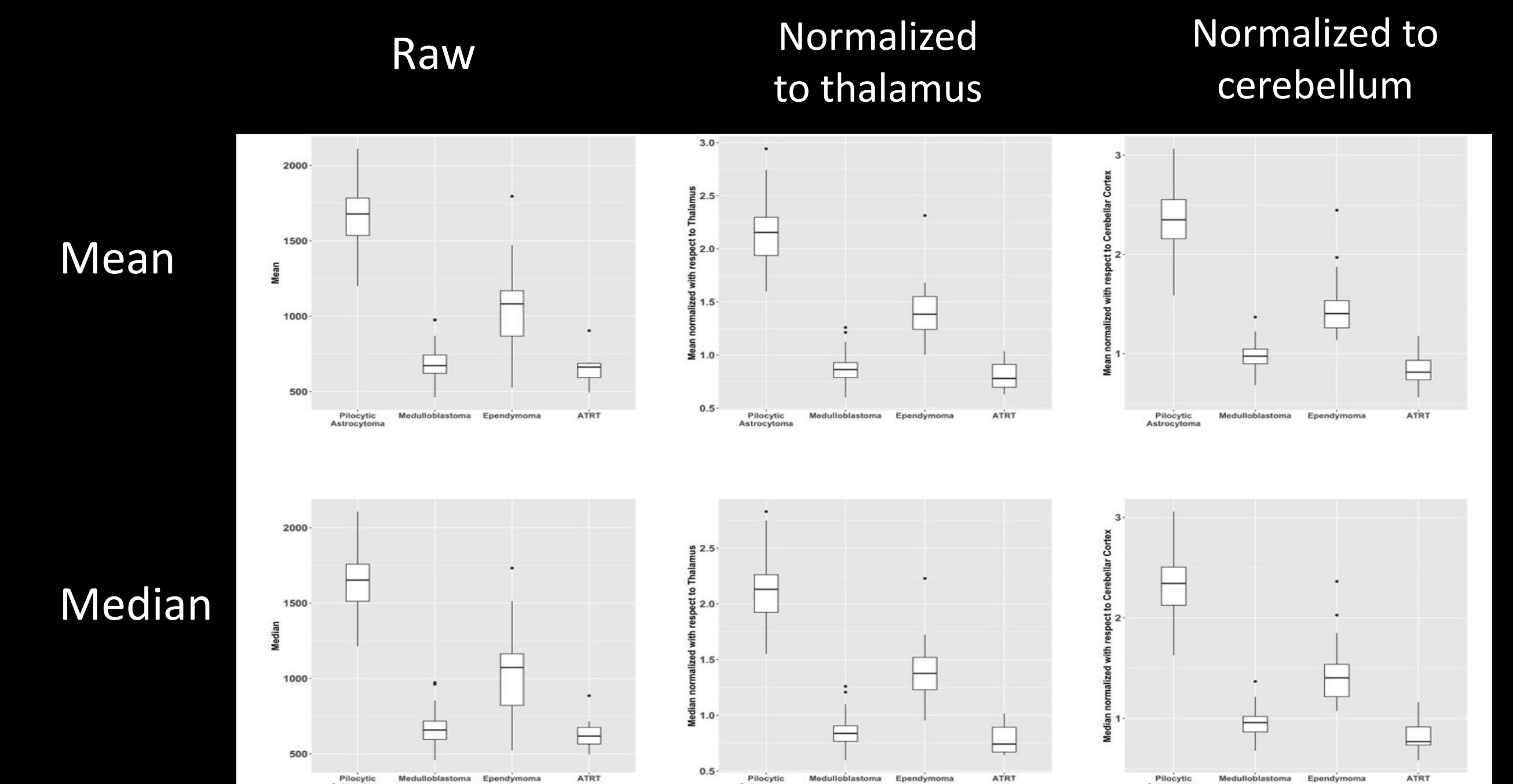
ADC map values vs. averaged number of pixels for each posterior fossa tumor type. ADC map values are depicted in the X axis. Averaged number of pixels (Y axis) were weighted to control for differences in group sample sizes.

ADC histogram metric values of the four most common pediatric posterior fossa tumors					
ADC histogram feature	Pilocytic Astrocytoma* (N=75)	Medulloblastoma* (N=59)	Ependymoma* (N=16)	ATRT* (N=13)	p value #
Entropy	4.1 (3.72-4.42)	3.48 (3.27-3.67)	3.67 (3.28-4.22)	3.64 (2.84-3.87)	<0.001
Minimum	1201.36 (1040.4-1358.83)	382.21 (308.55-445.39)	722.69 (534.93-791.69)	361.41 (284.27-412.1)	<0.001
10th percentile	1460 (1300-1620)	540 (500-580)	880 (659.09-1000)	500 (460-540)	<0.001
90th percentile	1940 (1780-2100)	820 (740-940)	1260 (1028.33-1360)	820 (780-860)	<0.001
Maximum	2523.73 (2260.76-2798.42)	1250.21 (1117.08-1408.5)	1661.34 (1271.08-1958.79)	1172.28 (1039.97-1487.76)	<0.001
Mean	1678.7 (1531.44-1800.61)	672.21 (619.54-744.37)	1082.22 (839.13-1169.32)	662.72 (592.44-687.12)	<0.001
Median	1653.26 (1509.21-1760.47)	658.82 (595.64-721.69)	1072.79 (795.4-1166.33)	617.8 (566.2-676.29)	<0.001
Skewness	0.76 (0.38-1.16)	0.85 (0.5-1.37)	0.72 (0.14-1.13)	0.78 (0.55-0.96)	0.616
Kurtosis	4.21 (3.3-5.95)	4.79 (3.2-6.37)	3.68 (2.76-5.48)	4.42 (3.58-5.1)	0.707

Data is reported as median (IQR); the unit for minimum, 10th percentile, 90th percentile, maximum, mean and median is  $10^{-6} \text{ mm}^2/\text{s}$   
 # P-value reported based on Kruskal-Wallis test  
 § p value < 0.05

ADC histogram metric values of the four most common pediatric posterior fossa tumors					
ADC histogram feature	Cut-off	AUC	95% CI	Sensitivity (%)	Specificity (%)
Minimum	$\leq 562.5 \times 10^{-6} \text{ mm}^2/\text{s}$	0.91	0.83-0.98	94.9	75
10th percentile	$\leq 740 \times 10^{-6} \text{ mm}^2/\text{s}$	0.88	0.78-0.97	100	68.7
90th percentile	$\leq 980 \times 10^{-6} \text{ mm}^2/\text{s}$	0.83	0.69-0.96	94.9	81.2
Maximum	$\leq 1408.5 \times 10^{-6} \text{ mm}^2/\text{s}$	0.70	0.56-0.85	76.3	75
Mean	$\leq 870 \times 10^{-6} \text{ mm}^2/\text{s}$	0.85	0.72-0.96	96.6	75
Median	$\leq 827.8 \times 10^{-6} \text{ mm}^2/\text{s}$	0.85	0.73-0.96	94.9	75
T-Minimum	$\leq 1.036$	0.75	0.66-0.84	71.2	86.7
T-10th percentile	$\leq 1$	0.96	0.9-1	93.2	93.3
T-90th percentile	$\leq 1.170$	0.99	0.98-1	96.6	100
T-Maximum	$\leq 1.438$	0.88	0.8-0.94	89.8	80
T-Mean	$\leq 1.001$	0.98	0.97-1	89.8	100
T-Median	$\leq 1.067$	0.98	0.96-1	94.9	93.3
C-Minimum	$\leq 0.993$	0.95	0.89-0.99	91.4	93.3
C-10th percentile	$\leq 1.064$	0.97	0.94-1	94.9	93.3
C-90th percentile	$\leq 1.270$	0.94	0.87-0.99	93.2	86.7
C-Maximum	$\leq 1.588$	0.75	0.63-0.87	78	66.7
C-Mean	$\leq 1.108$	0.97	0.94-0.99	89.8	100
C-Median	$\leq 1.066$	0.97	0.95-1	88.1	100

T : normalized to thalamus  
 C : normalized to cerebellar cortex



Box and whisker plots of median and inter-quartile range demonstrate significant differences between all four common posterior fossa tumors, except Medulloblastoma versus ATRT.

## Conclusion

We successfully applied the histogram analysis of the ADC map in a large group of pediatric PF tumors and successfully differentiated tumor types as well as provided critical cutoff values.

